EUROPEAN COMMISSION

Community Research

RAPHAEL

Contract Number: 516508 (FI6O)

DELIVERABLE (D-ML3.19)

Development of modelling methods for graphite behaviour – micro-structural model developments

Author(s): **Graham HALL**

Reporting period: e.g. 15/04/2005 – 14/04/2010

Date of issue of this report : 09/04/2010

Start date of project : **15/04/2005** Duration : **60 Months**

Project co-funded by the European Commission under the Euratom Research and Training Programme on Nuclear Energy within the Sixth Framework Programme (2002-2006)		
Dissemination Level (place an X in the appropriate cell)		
PU	Public	
RE	Restricted to the partners of the RAPHAEL project	
CO	Confidential, only for specific distribution list defined on this document	**X**

Distribution list

Person and organisation name and/or group	Comments
SP4 ML WP3 Partners	

ReActor for Process heat, Hydrogen And ELectricity generation (RAPHAEL)		
Sub-project: SP-ML **Work package:** 3	**RAPHAEL document no:** RAPHAEL 1004 D ML3.19	**Document type:** D=Deliverable / M=Minute / P=Progress report / S=Support
Issued by: Uni Man (UK) **Internal no.:** NGRG R		**Document status:** Final

Document title

Development of modelling methods for graphite behaviour – micro-structural model developments

Abstract

In the graphite modelling sub-task within the RAPHAEL Integrated Project, it was suggested that the computed X-ray tomography technique could provide further insight into the irradiation-induced microstructural changes in graphite, and aid in the development of microstructural models of graphite. This was investigated within the original timescale of the project, but an extension of the project has permitted further investigation. The feasibility of using this technique was examined further using two specimens that had been X-ray tomography scanned and then irradiated in the High Flux Reactor (Petten, the Netherlands) were returned to the University of Manchester for a post-irradiation computed X-ray tomography scan. Qualitative comparisons of the tomography data, before and after irradiation, indicated that irradiation-induced microstructural (pore) changes could be detected in the tomography data. This gave some confidence that the computed X-ray tomography technique can be used to gain further insight into the microstructural changes within the graphite and also be used in the development of models. To gain quantitative results, additional X-ray tomography scans at higher resolutions would be needed on further samples. This work should be performed in a future Framework .

Revisions

Rev.	Date	Short description	Author	WP Leader	SP Leader	Coordinator
00			Name, Organisation *Signature*	Name, Organisation *Signature*	Name, Organisation *Signature*	Name, Organisation *Signature*
01	09/04/2010	Final issue	G Hall, Uni Man			

Contents

1 Introduction

The European Commission's 6th Euratom Framework Programme (RAPHAEL-IP) incorporated numerous sub-projects that supported research co-operation and integration of research efforts in the nuclear fission and fusion area. One such sub-project was the Materials Sub-project (SP-ML). Each of the sub-projects were subdivided into work packages, with Work Package 3 (WP3) of SP-ML being concerned with graphite materials for the very-high temperature reactor (VHTR).

There were 4 tasks within WP3:

- Task 1 – continuation of 750°C irradiation tests.
- Task 2 – graphite irradiation test at higher (>950°C) VHTR temperatures.
- Task 3 – corrosion and heat-up test.
- Task 4 – graphite modelling.

The final task (Task 4) was undertaken by the University of Manchester and was summarised as[1]:

> *For the longer term development of graphites and to minimise the extent of future irradiation testing, work will also be carried out on an investigation of microscopic modelling methods for prediction and assessment of graphite behaviour making use of micrographs and tomography images of graphites used in the RAPHAEL-IP tests.*

with the added note that it was:

> *essential that its behaviour is fully understood and investigated up to at least the peak dose and over the appropriate temperature ranges.*

The programme for Task 4[2] included the identification and selection of graphite properties, a survey of possible modelling techniques, a stage report of the first two sub-tasks, preliminary application of these techniques, a review of the initial application and selection of preferential techniques, development and re-application of the techniques, and a final report on the task. A number of reports[3-6] detail the work, overall findings, and recommendations from this task.

To take advantage of the extension year, it was agreed the task could be extended to complete the post irradiation examination of the graphite specimens irradiated in HFR (High Flux Reactor), Petten, The Netherlands. This extension gave the opportunity to further investigate the use of computed X-ray tomography data in the microstructural modelling of nuclear grade graphite

2 Computed X-ray tomography

Computed X-ray tomography (CT) has been used in the medical field for many years, and was investigated as a characterisation technique for nuclear graphite in the 1980s[7, 8]. However, it has only recently been re-applied to the study of graphite microstructure.

Computed X-ray tomography is a non-destructive technique that provides a means to examine the 3D microstructure of a material. In the case of an irradiation programme, a specimen can be removed for inspection and then placed back in the reactor for further irradiation. The CT technique involves sending an X-ray beam through a sample and recording the transmitted beam using a detector, usually a CCD (charge-coupled device) camera (**Figure 1**). The ratio of transmitted to incident photons is related to the integral of the absorption coefficient of the material along the path that the photons made through the material[9]. Using an empirical law, the absorption coefficient can be related to the density, the atomic number, and in certain cases, the energy. The resulting image is a projection of a volume in a 2D plane. The most popular method of obtaining a 3D image is to obtain radiographs whilst rotating the sample between 0° and ~180°. An algorithm (such as the filtered back-projection algorithm) can then be used to form or reconstruct the 3D volume from the 2D radiographs.

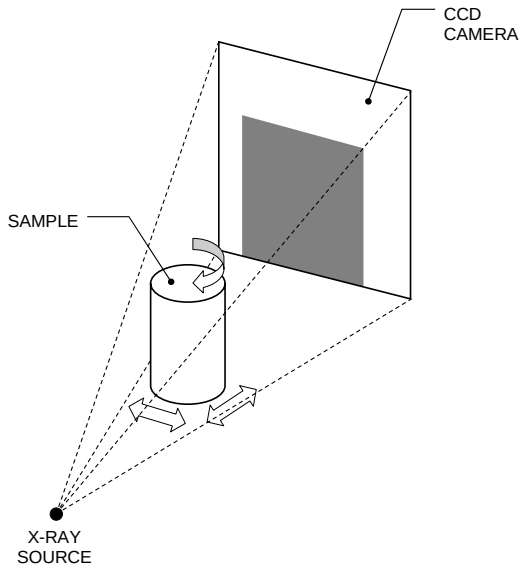

Figure 1 Schematic of X-ray tomography using a micro-focus X-ray tube source.

There are two different X-ray sources used in X-ray tomography. A micro-focus X-ray tube produces a polychromatic divergent beam whilst a synchrotron radiation source is able to produce either a polychromatic or monochromatic beam that is parallel to the

detector. The micro-focus X-ray tube arrangement is usually found in the smaller scale devices such as the laboratories at the University of Manchester.

When using an X-ray tube source, the sample is placed between the source and detector. The sample should fit the field of view of the detector, and thus a compromise must often be made between the sample size and the spatial resolution (this also depends upon the detector i.e. number of pixels in the CCD camera). As the beam is polychromatic (comprises of rays of different energies), quantitive analysis requires calibration and is only accurate in single-phase materials.

2.1.1 Outputs from tomography

The CT technique has the ability to give a number of characteristics of a sample in a non-destructive way. The porosity can be examined in 3D terms but a number of factors have to be considered. The sample size and CCD camera used affects the resolution of the 3D image. If a ø10mm sample is scanned using a CCD camera with a resolution of 1024 × 1024 pixels, the resulting reconstructed volume will have a resolution of ~11µm i.e. each 3D pixel (a voxel) will be ~11 × 11 × 11µm. Thus, the smallest porosity or characteristics that can be identified will be ~11µm. If however, a smaller sample is used (ø5mm) the voxel size will reduce (~6µm) but the representative volume will have reduced also. It is therefore a trade between sample size and resolution, although the resolution may also be increased by having a CCD camera with an increased pixel resolution i.e. 2048 × 2048 pixels.

The results will also be affected by the processing of the reconstructed volume. To separate or segment the volume, a greyscale or threshold value is often used. The value used may not be obvious and may cause uncertainty in the results. For example, the porosity in a sample may be segmented from the bulk material using a threshold value (**Figure 2**). However, the amount of porosity can be highly dependent upon what value is used.

When the sample is single phase, it is possible to obtain the density distribution and bulk density of the sample. This requires calibration of the CT equipment and material under examination so that the greyscales in the reconstructed volume can be related to a density value.

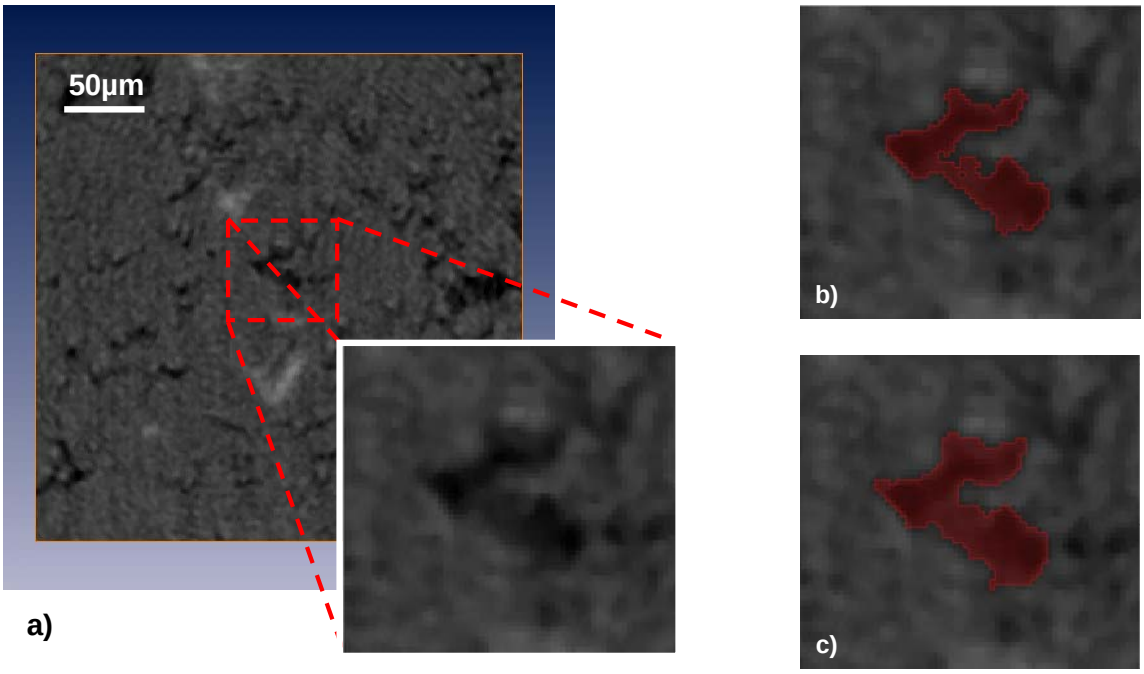

Figure 2 Effect of threshold value on the segmentation process; a) reconstructed 3D volume of a graphite sample (8 bit, 255 greyscale); b) segmentation of pore using threshold value of 36; c) segmentation of pore using threshold value of 42.

2.2 CT data in microstructural modelling

The X-ray computed tomography data has the opportunity to aid the development of nuclear graphite microstructural models in a number of ways. The CT data could be used to support some of the assumed mechanisms behind the irradiation-induced changes in bulk graphite dimensions and Young's modulus. The main driving forces of these changes are postulated to be the crystallite dimensional changes in combination with the closure of small-scale porosity. If this pore closure could be detected in the CT data, it would give some support to the models based upon this mechanism. If pore closure was confirmed to be an important part of the microstructural changes, the distribution (size and morphology) of the pores could be obtained from the CT data and implemented into the microstructural model such as the hierarchical/embedded approach investigated within this project[6]. Alternatively, models that encompass the necessary range of pores could be created directly from the CT data (reproduction approach[6]). In order to determine if CT data could provide such information, the CT scans of two graphite samples in the pre- and post-irradiation condition were examined.

3 Graphite samples examined

A range of nuclear graphite grades have been, and are being, irradiated in HFR as part of the FP5 and FP6 Integrated Projects. The irradiation experiments were divided into four separate programmes that covered the range of doses and temperatures deemed to encompass the needs of future HTR designers and operators. The first of these irradiation programmes (INNOGRAPH-1A) commenced in the FP5 Integrated project and was designed to give data at low to medium fast neutron fluences at 750ºC. A selection of graphite grades were included in the irradiation programme (Table 1) and prior to being irradiated, the material and dimensional properties of the specimens were measured by NRG, Petten, and 54 of the specimens were CT scanned at the University of Manchester.

After irradiation, the dimensional and material properties of all of the specimens were re-measured by NRG, and two specimens (S084 and U019) that had been CT scanned prior to irradiation were sent to the University of Manchester for another CT scan. The details of these specimens are given in Table 2.

Table 1 Graphite grades in the INNOGRAPH-1A irradiation programme.

Grade	Supplier	Coke	Manufacture
IG-110	Toyo	petroleum	iso-moulding
IG-430	Toyo	pitch	iso-moulding
NBG-10	SGL	pitch	extrusion
NBG-20	SGL	petroleum	extrusion
NBG-25	SGL	petroleum	iso-moulding
PCEA	GrafTech	petroleum	extrusion
PCIB	GrafTech	petroleum	iso-moulding
PPEA	GrafTech	pitch	extrusion

Table 2 Details of specimens S084 and U019.

	S084		U019	
grade	NBG-10		PCEA	
location†	edge		centre	
orientation‡	against grain		against grain	
fluence (dpa)	0	9.16	0	8.66
irradiation temperature (ºC)		750		750
density (g/cm^3)	1.824	1.910	1.810	1.924
dimensional change (%)		-1.35		-1.98
dynamic Young's modulus (GN/m^2)	12.8	27.9	11.0	23.4

†Where the specimen was machined from with respect to the graphite billet.

‡Alignment of the grains with respect to the longitudinal axis of the specimen.

4 CT of the graphite specimens

Prior to irradiation, the graphite specimens (S084 and U019) were CT scanned at the University of Manchester using an X-tek HMX-255 laboratory CT machine. The operator was able to calibrate the scan settings, thus allowing the greyscale distribution of the CT scans to be consistent between the specimens. The resolutions of the scans were also consistent between the two specimens at ~8.4µm/voxel. Examples of images from the three-dimensional CT reconstruction are shown in **Figure 3**.

After irradiation, the same specimens were sent to the University of Manchester for another CT scan (**Figure 4**). However, the CT machine had been replaced with a Metris X-tek XTH-225. Although this new CT machine can give the same resolution as before, the resolutions of the post-irradiations scans were lower than the pre-irradiation scans at ~14.1µm/voxel for S084 and ~11.2µm/voxel for U019. The ability to calibrate the scanning settings appears to be no longer possible and the CT machine now determines automatically what are perceived to be the optimum settings for that particular scan.

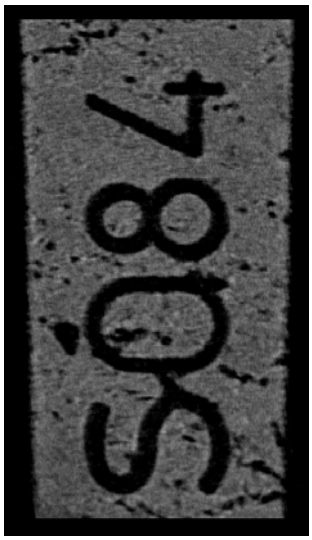

a) vertical slice through S084

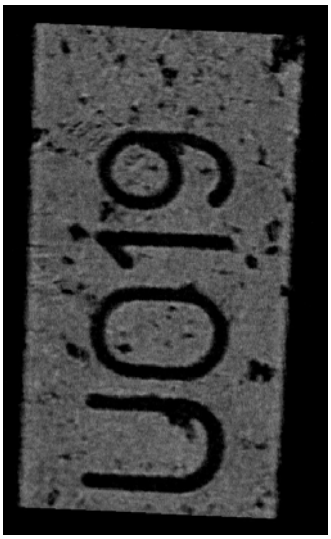

b) vertical slice through U019

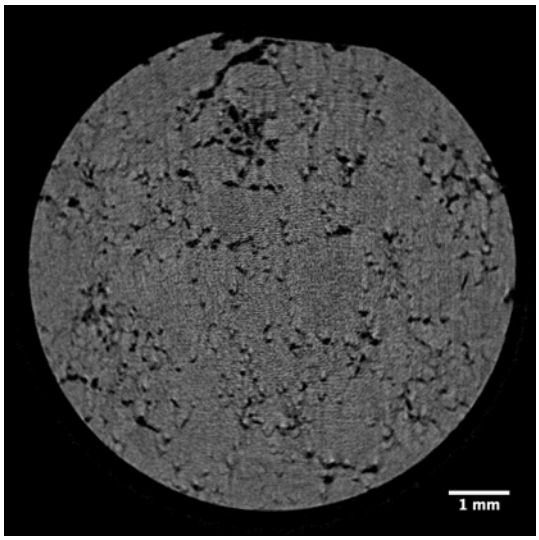

c) horizontal slice through S084

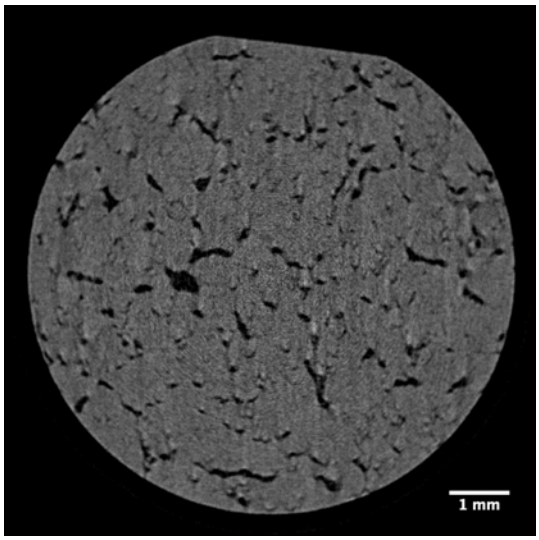

d) horizontal slice through U019

Figure 3 Images from the CT reconstruction of specimens S084 and U019 prior to irradiation.

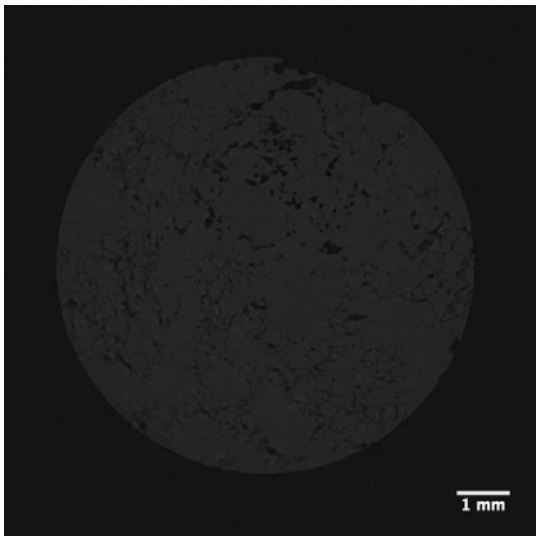

a) horizontal slice through S084

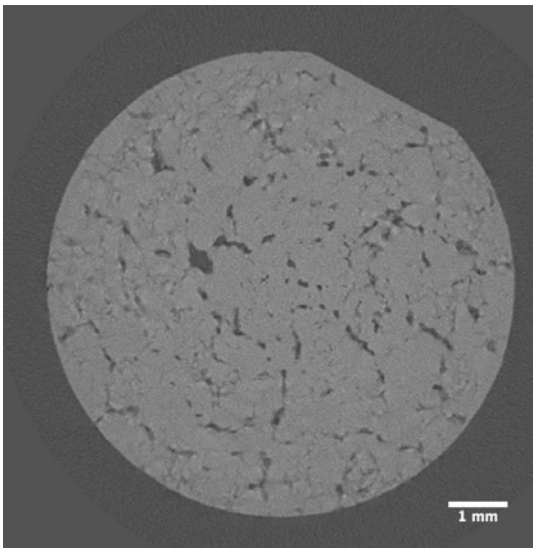

b) horizontal slice through U019

Figure 4 Images from the CT reconstruction of specimens S084 and U019 after irradiation.

4.1 Comparison of CT data

Visual comparison of the pre-irradiation scans (**Figure 3**) showed that the greyscale distributions of the two samples were similar, and this was further confirmed by plotting the greyscale distributions of the CT volumes (**Figure 5**). Comparison of the greyscale distributions of the post-irradiation scans showed that the distributions were significantly different from each other, and different from the pre-irradiation scans (**Figure 5**). Irradiation is expected to cause a shift to the right (and then back to the left) in the greyscale distribution due to the increase (and then decrease) in graphite density with irradiation. However, the large differences observed here were caused by the change in the CT machine used. This was important as the repercussion was that the pre- and post-irradiation scans could not be compared directly and any change in density of the specimens with irradiation could not be examined at all.

Although the density changes could not be examined, it was still possible to examine the effect of irradiation on the porosity with the graphite specimens. However, as the greyscale distributions were inconsistent, the porosity comparisons must be taken as being qualitative. In previous CT investigations[10, 11], a greyscale threshold level based upon a density value was used. The same density value and greyscale threshold level could be used when the graphite had been modified in some way, whether it was by oxidation or irradiation. This would give quantitative results. In this case, however, a standard greyscale or density value could not be used and the investigator had to use a judgement-based threshold value. Thus, the comparisons can only at best, be considered to be qualitative.

Before any analysis of the porosity was conducted, the CT scans of S084 (unirradiated) and U019 (unirradiated and irradiated) were rescaled so that the resolutions of the scans were all approximately the same (~14µm/voxel). Two sub-volumes (300 × 300 × 300 voxels) were then cropped from each of the rescaled volumes. These sub-volumes were segmented using a threshold value that gave visually the correct division between porosity and graphite. The resulting segmented sub-volumes were then analysed using a Matlab routine that categorises and measures the porosity within a segmented volume[10].

The Matlab routine calculated the porosity content within the segmented sub-volumes, and also separated the porosity into two main groups; connected and isolated porosity. The main characteristic of the connected porosity was its tortuosity, with it being similar to a dendritic shape with many branches, whereas the isolated pores were more compact in shape. The fraction of connected and isolated porosity was also calculated. Furthermore, the size distribution of the isolated pores was calculated for each sub-volume. The average of the two sub-volumes for each CT scan was then calculated (Table 3 and **Figure 6**).

The results of the porosity content analyses (Table 3) suggested that there were slight differences in the porosity content between the two specimens, and possibly grades. The specimen S084 had slightly more porosity than specimen U019, with S084 having a slightly higher fraction of connected porosity. This contrary to the measured properties (Table 2) as a graphite with a higher porosity content would be expected to have a lower unirradiated density and Young's modulus, and a greater amount of dimensional change. However, specimen S084 had a higher unirradiated density and Young's modulus, and less dimensional change compared to U019. The likely cause of this was the segmentation process which assumed that both pre-irradiation CT scans were done at exactly the same conditions. This was not the case and there would have been variations in the energy spectrum of the X-ray beam. Thus, there were differences in the greyscale distributions not due to differences in the specimens themselves, and as the segmentation process is sensitive to the greyscale distribution, there could have been an effect on the porosity. A way of determining, and possibly correcting for, the amount of fluctuation in energy and greyscale would be to include the same calibration specimen (such as a small piece of highly oriented pyrolytic graphite) with each specimen scan.

Another possible discrepancy was related to the fact that the specimens were from different regions in the billet, which could cause a difference in the porosity. It would be expected that an edge specimen such as S084 would have a higher density and lower porosity content than a centre specimen such as U019 due to the impregnation stage in manufacture. However, this was not the case with respect to the CT data.

The results did not give a clear indication of how the total amount of porosity is changing with irradiation as specimen S084 demonstrated a small reduction in total

porosity with irradiation whilst specimen U019 demonstrated a similar size of increase in porosity. However, both specimens did show a decrease in connected porosity fraction (and an increase in isolated porosity fraction) with irradiation, albeit larger in specimen S084. Such a change could be attributed to the irradiation-induced dimensional changes causing the closure of some parts of the connected porosity, thus forming more isolated pores.

Comparison of the isolated porosity distributions of the two specimens before and after irradiation supported there being differences in the isolated pore content (**Figure 6**). Both specimens showed a decrease in the quantity of pores below ~40µm equivalent diameter. This implies that it is the small-scale pores that are closing with irradiation, and that the large pores may only be reducing in size. However, higher resolution CT volumes obtained using the same CT settings would be required to confirm this.

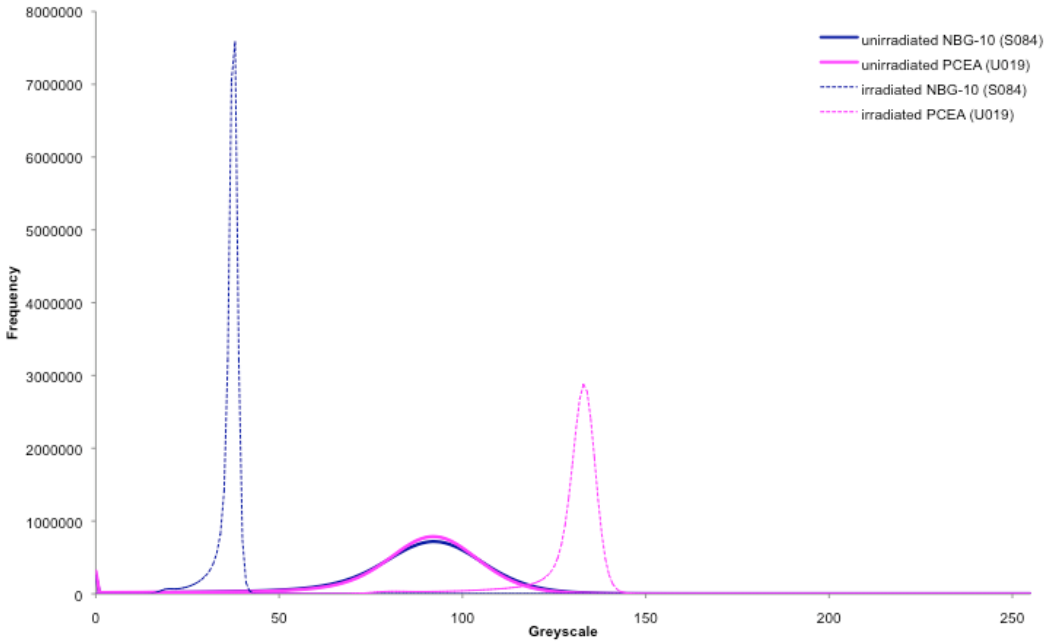

Figure 5 CT greyscale distributions of the specimens S084 and U019, pre- and post irradiation.

Table 3 Porosity content calculated from the CT scans of specimens S084 and U019.

Specimen	Condition	Porosity (% volume)	Connected porosity (% of porosity)	Isolated porosity (% of porosity)
S084	unirradiated	7.1	53.8	46.2
S084	irradiated	6.8	44.6	55.4
U019	unirradiated	6.7	49.8	50.2
U019	irradiated	7.0	47.9	52.1

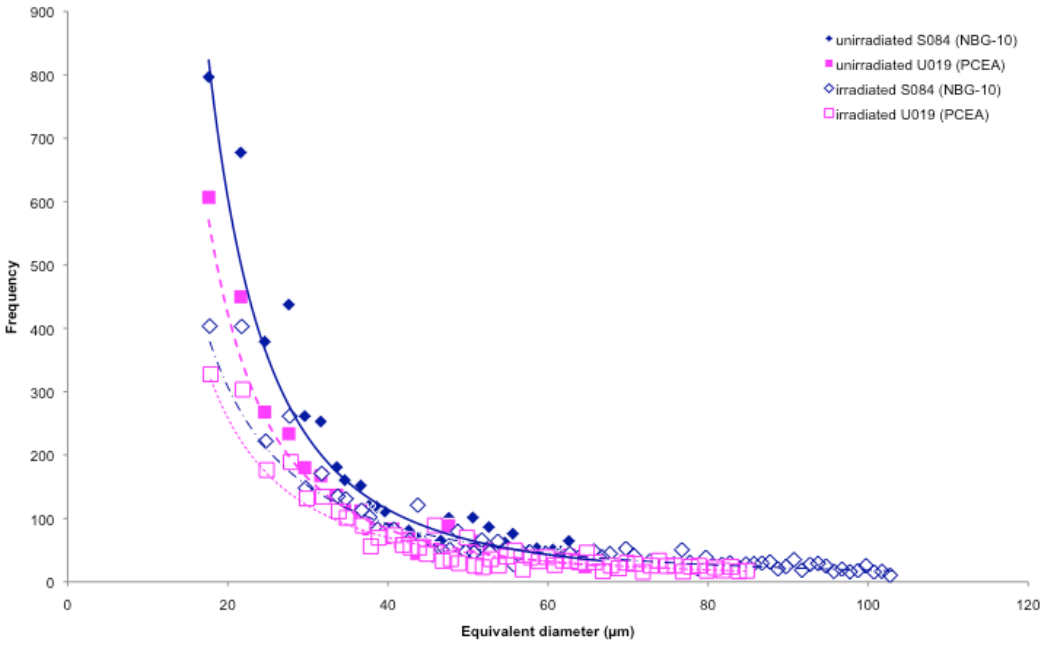

Figure 6 Size distribution of isolated porosity of specimens S084 and U019, pre- and post irradiation.

5 Application to microstructural modelling

Although the analysis and comparison of the pre- and post-irradiation CT data did not give definitive support to the postulated microstructural mechanisms, it did give an indication that there was some form of pore closure with irradiation. If the porosity range and morphologies of importance to the materials properties changes are included, it is perceived that reproduction type models could be constructed. The observed differences in pore content and pore distribution between the specimens examined provides support that CT data could be used to model the differences in the bulk properties of different grades, as long as the cause of the property differences are linked to porosity.

However, for the CT data to be of use for modelling purposes, further higher-resolution and quantitative comparisons would have to be made. The comparisons made here were only for two specimens, and a range of specimens needs to be considered. Thus, CT data obtained pre- and post-irradiation on a range of specimens, that were the same with respect to the CT settings and reconstruction methods used, would provide further support to the mechanisms and allow for further development of the microstructural models.

6 Conclusions

- A year's extension to the original timescale of the RAPHAEL Integrated Projected allowed for the further investigation of the use of computed X-ray tomography data in the microstructural modelling of nuclear grade graphite.

- Computed X-ray tomography data was postulated to have the capability to provide support to the assumed microstructural changes (porosity closure) behind the irradiation-induced dimensional and Young's modulus changes in bulk graphite. If this mechanism was supported, the relevant pore size and morphology distribution could possibly be extracted from the data and implemented into a microstructural model, or a model could be created from the computed X-ray tomography data directly.

- The feasibility of gaining such knowledge and data was investigated by analysing and comparing the computed X-ray tomography data for two graphite specimens before and after irradiation in the High Flux Reactor, Petten, the Netherlands. The specimens examined were S084 (NBG-10) and U019 (PCEA), both of which were irradiated to ~9dpa at 750ºC.

- Although the specimens were scanned at the University of Manchester, the X-ray tomography machine used pre- and post-irradiation differed. The consequence of this was that the computed X-ray tomography data of the specimens before and after irradiation were not directly comparable. Also, due to restrictions with the new tomography equipment, the two post-irradiation scans were not comparable to each other. Thus, only qualitative statements can be made from the data comparisons.

- Comparison of the porosity content of the two samples indicated that the specimens had different pore size distributions and that specimen S084 contained more porosity than specimen U019. Both specimens showed a reduction in connected porosity with irradiation, and a reduction in small-scale (<~40µm equivalent diameter) isolated pores with irradiation.

- Further evidence from the examination of a range of specimens is required, in particular computed X-ray scans at higher resolution using the same equipment on pre- and post-irradiation samples, where the reconstruction process can be controlled. Only then can quantitative assessments be made.

- When such investigations are completed, it may be possible to identify the porosity closure mechanism, and determine the pore distribution of importance, directly from the computed X-ray tomography data. These could then be applied in the microstructural modelling of nuclear grade graphite.

7 References

[1] Buckthorpe D. *Sub-project ML: Materials Development, SP-ML-WP3: Graphite Materials, Graphite Materials - Work plan for first 18 months*. NNC Limited, 12820/TR/001 Issue 01, 2005.

[2] Hall G. *European Commission 6th Euratom Framework Programme 2002-2006, Sub-project ML: Materials Development, SP-ML-WP3: Graphite Materials, Task 4 programme*. Nuclear Graphite Research Group, The University of Manchester, NGRG P162 Issue 1, 2005.

[3] Hall G. *Status of development of modelling method for graphite*. RAPHAEL IP, European Commission, RAPHAEL-0604-D-ML3.5-1, 2006.

[4] Hall G. *Graphite modelling progress report*. RAPHAEL IP, European Commission, RAPHAEL-0704-P-ML3.5-1, 2007.

[5] Hall G. *Graphite modelling progress report*. RAPHAEL IP, European Commission, RAPHAEL-0804-P-ML3.5-1, 2008.

[6] Hall G. *Graphite modelling progress report*. RAPHAEL IP, European Commission, RAPHAEL-0904-D-ML3.11, 2009.

[7] Ioka I, Yoda S, Fujii M, Oku T and Tanaka T. *Non-Destructive Testing of Graphites Using X-Ray Computed Tomography Scanner*. Nihon-Genshiryoku-Gakkai Shi (J. At. Energy Soc. Jpn.). 1986 June, 28(6), pp. 534-542.

[8] Ioka I and Yoda S. *Measurements of the Density Profile in Oxidized Graphite by X-Ray Computed Tomography*. Journal of Nuclear Materials. 1988 Jan., 151(2), pp. 202-208.

[9] Salvo L, Cloetens P, Maire E, Zabler S, Blandin JJ, Buffière JY, Ludwig W, Boller E, Bellet D and Josserond C. *X-ray micro-tomography an attractive characterisation technique in materials science.* Nuclear Instruments and Methods in Physics Research B. 2003, 200, pp. 273-286.

[10] Babout L, Mummery PM, Marrow TJ, Tzelepi A and Withers P. *The effect of thermal oxidation on polycrystalline graphite studied by X-ray tomography.* Carbon. 2005, 43, pp. 765-774.

[11] Babout L, Marsden BJ, Mummery PM and Marrow TJ. *Three-dimensional characterization and thermal property modelling of thermally oxidized nuclear graphite*. Acta Materialia. 2008, 56(16), pp. 4242-4254.